Adsorption of Lead Ions from Aqueous Phase on Mesoporous Silica with P-Containing Pendant Groups

ARTICLE *in* ACS APPLIED MATERIALS & INTERFACES · SEPTEMBER 2015

Impact Factor: 6.72 · DOI: 10.1021/acsami.5b06951

5 AUTHORS, INCLUDING:

Chamila Gunathilake
Kent State University
13 PUBLICATIONS **27** CITATIONS
SEE PROFILE

Murthi S Kandanapitiye
Kent State University
6 PUBLICATIONS **6** CITATIONS
SEE PROFILE

Songping D Huang
Kent State University
113 PUBLICATIONS **2,649** CITATIONS
SEE PROFILE

ACS APPLIED MATERIALS & INTERFACES

Research Article

www.acsami.org

Adsorption of Lead Ions from Aqueous Phase on Mesoporous Silica with P-Containing Pendant Groups

Chamila Gunathilake,[†] Murthi S. Kadanapitiye,[†] Oksana Dudarko,[‡] Songping D. Huang,[†] and Mietek Jaroniec*[,†]

[†]Department of Chemistry and Biochemistry, Kent State University, Kent, Ohio 44242, United States

[‡]Chuiko Institute of Surface Chemistry NAS of Ukraine, 17, General Naumov Street, Kyiv, 03164, Ukraine

Supporting Information

ABSTRACT: Mesoporous silica materials with hydroxyphosphatoethyl pendant groups (POH-MS) were obtained by a two-step process: (1) block copolymer Pluronic P123-templated synthesis of mesoporous silica with diethylphosphatoethyl groups (DP-MS) by co-condensation of diethylphosphatoethyl triethoxysilane (DPTS) and tetraethylorthosilicate (TEOS) under acidic conditions and (2) conversion of diethylphosphatoethyl into hydroxyphosphatoethyl groups upon suitable treatment with concentrated hydrochloric acid. The DP-MS samples obtained by using up to 20% of DPTS featured hexagonally ordered mesopores, narrow pore size distribution and high specific surface area. Conversion of DP-MS to mesoporous silica with hydroxyphosphatoethyl groups (POH-MS) resulted in the enlargement of the specific surface area, total porosity, and microporosity. High affinity of hydroxyphosphatoethyl groups toward lead ions (Pb^{2+}) makes the POH-MS materials attractive sorbents for lead ions, which is reflected by high lead uptake reaching 272 mg of Pb^{2+} per gram of POH-MS. This study shows that the simple and effective co-condensation strategy assures high loading of P-containing groups showing high affinity toward lead ions, which is of great importance for removal of highly toxic lead ions from contaminated water.

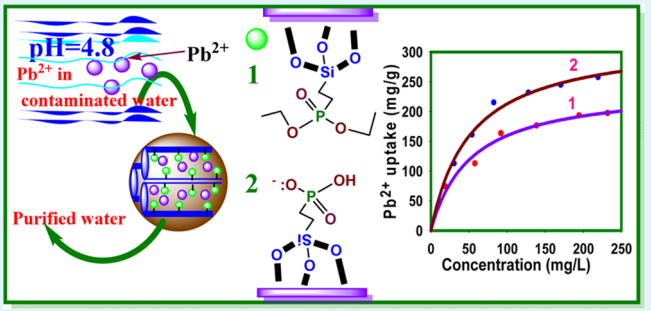

KEYWORDS: *lead, adsorption, mesoporous organosilica, diethylphosphatoethyl triethoxysilane*

INTRODUCTION

Release of pollutants such as heavy metal ions and dyes by chemical industry into aqueous environment significantly threatens human health. Therefore, an effective control of industrial emissions and capture of the pollutants exceeding the established norms by the U.S. Environmental Protection Agency (EPA) is needed. Silica and activated carbons are widely used to remove toxic substances from polluted water. For instance, the properly modified ordered mesoporous silica (OMS) materials have been already investigated as adsorbents for heavy metal ions. Attachment of proper functional groups to the silica surface via co-condensation or postsynthesis grafting has been used to generate specific binding sites in mesopores of these materials. The creation of binding sites for heavy metal ions on the silica surface is usually based on the hard−soft acid−base theory. For instance, silica with attached thiol groups shows high affinity toward Hg^{2+} ions. Ligands with amine and thiol groups have been introduced to the mesopores of MCM-41and SBA-15[1−5] to achieve high surface coverage of these groups; the resulting materials showed an excellent binding affinity, large capacity, good stability, and high selectivity for many heavy metal ions. Ligands containing sulfur (thiol, thiourea, thioether),[1−3,6,7] nitrogen (aminopropyl, ethylenediamine),[8−10] and carboxylic acid[11] groups have been applied effectively for adsorption of various metal ions such as Hg^{2+}, Cu^{2+}, Ni^{2+}, Cr^{3+}, Fe^{3+}, Cd^{2+}, and Ni^{2+} under different experimental conditions. For instance, Feng and co-workers synthesized mercaptopropylsilyl modified OMS for treatment of contaminated water with Hg^{2+}, Pb^{2+}, Ag^{+}, and Cr^{3+} at different pH conditions.[1] They observed that Hg^{2+} and Ag^{+} initial concentrations were reduced well below the EPA limit after adding OMS with mercaptopropylsilyl groups. This material was shown to be stable at moderately high temperatures in water and air and suitable for regeneration under mild acidic conditions. One of the great advantages of this material is the relatively small size of mesopores (below 20 nm), which prevents activity of larger bacteria toward producing deadly methyl mercury (CH_3Hg). A direct synthesis of cubic benzene-silica containing mercaptopropyl groups was reported by the Hao group; this material was shown to be a better adsorbent for Hg^{2+} and Ag^{+} as compared to Cd^{2+}, Co^{2+}, and Pb^{2+}.[2] This study revealed a shift of the ^{13}CNMR peak corresponding to the carbon atom neighboring to the thiol group after mercury and silver attachment but not in the case of other heavy metal ions.

Received: July 30, 2015
Accepted: September 29, 2015

DOI: 10.1021/acsami.5b06951
ACS Appl. Mater. Interfaces XXXX, XXX, XXX−XXX

This behavior was elucidated on the basis of Pearson's theory of hard−soft acid−base compounds, according to which the hanging mercaptopropyl groups are soft Lewis bases and show higher affinity toward soft Lewis acids such as Ag^+ and Hg^{2+} but much smaller toward moderately hard Lewis acids such as Co^{2+}, Cd^{2+}, and Pb^{2+}. Benzoyl thiourea-modified mesoporous silica was used for Hg^{2+} adsorption by the Jaroniec group.[3] They synthesized this material by incorporating an aminopropyl group into MCM-41 and then converting it to a 1-benzoyl-3-isopropylthiourea group through nucleophilic reaction between an amine group and benzoyl isothiocyanate. They further demonstrated that 1-benzoyl-3-isopropylthiourea ligand shows a high affinity toward Hg^{2+} while the remaining NH_2 groups interact weakly with Hg^{2+}. Removal of Ni^{2+}, Cd^{2+}, and Pb^{2+} by amino-functionalized mesoporous silica was studied by Heidari et al.,[10] who showed that pH of the medium is an important factor in adsorption of heavy metal ions. An increase in the adsorption efficiency was observed with increasing pH from 1.5 to 5.0 because pH influences electrostatic interactions of ions with NH_2 groups as the protonated amine groups ($-NH_3^+$) transform to deprotonated groups at higher pH (NH_2 or NH^-), which alters the number of available binding sites. Shengue and co-workers studied thiol-functionalized MCM-41 for Cu^{2+}, Pb^{2+}, Ag^+, and Cr^{3+} removal.[7] They demonstrated that the adsorption capacity of Cu^{2+}, Pb^{2+}, Ag^+, and Cr^{3+} ions on the thiol-modified MCM-41 is higher at higher temperature.

In addition to the aforementioned chelating groups, phosphonic acid-based precursors such as diethylphosphatoethyl triethoxysilane have attracted significant attention among environmental researchers especially in the field of separation of rare earth elements and actinides.[12−17] Soft-templated OMS materials attracted also a lot of attention.[18−24] These ordered mesostructures are easily accessible for adsorption of heavy metal, lanthanide, and actinide ions. For instance, adsorption of U^{6+}-containing species by diethylphosphatoethyl surface groups is governed through the complex coordination chemistry. Recently, Pablo and co-workers synthesized 2D hexagonally ordered SBA-15 and 3D cubic KIT-6 OMS materials and grafted them with P-containing groups; these materials adsorbed 54−56 mg of U per gram and could be regenerated under mild acidic conditions.[12] Yuan et al. reported one-pot cationic surfactant-templated synthesis of analogous sorbents by using diethylphosphatoethyltriethoxysilane (DPTS) and tetraethylorthosilicate (TEOS) and obtained the maximum sorption capacity of 303 mg of U per gram of sorbent with fast equilibrium time.[14] Modeling of the binding of heavy metal ions (Cu^{2+}, Cd^{2+}, Co^{2+}, Pb^{2+}) with hydroxyphosphate groups present on activated carbon was reported by Puziy et al.[25] On the basis of the metal ion binding constants, they proposed the formation of monodentate charged complexes with a deprotonated phosphoric acid group. Incorporation of the aforementioned group into inorganic frameworks resulted in the development of hybrid materials having well-defined porosity and unique surface properties that are versatile, robust, and hydrothermally stable. Among many toxic metal ions discussed above, our attention has been directed toward lead species, which are discharged to the aquatic environment through many industrial processes such as textile dying, petroleum refining, ceramic and glass manufacturing, and the battery industry.[26−30] Lead ions can significantly impact mankind's health. For instance, it is possible to have some symptoms such as mental disturbance, retardation, semi-permanent brain damage, renal function hypertension, lung damage, kidney failure, and hepatic injury when people are exposed to high doses of lead ions for a prolonged time period.[26−30] Thus, it is worthy to explore the development of new sorbents for the capture of lead ions.

Herein, diethylphosphatoethyltriethoxysilane (DPTS) and tetraethylorthosilicate (TEOS) were employed to prepare mesoporous organosilica with diethylphosphatoethyl surface groups [$-P{=}O(OC_2H_5)_2$]. Next, these groups were converted to hydroxyphosphatoethyl [$-P{=}(O)\ (OH)_2$] groups using concentrated HCl (see Figure S1 in the Supporting Information), which are more favorable for chelating lead ions under suitably adjusted pH conditions. So far, this type of material was often boiled in concentrated hydrochloric acid or treated under different conditions to transform phosphonate ester functionality $-PO(OEt)_2$ to $-PO(OH)_2$.[22,23,31] The co-condensation method was employed for achieving a high concentration of the aforementioned organic groups assuring large sorption capacities of metal ions as compared to those obtained for analogous postgrafted materials.[32] This study shows that highly efficient sorbents for sorption of heavy metal ions can be developed by using proper functional organosilanes, biodegradable, and inexpensive triblock copolymer templates (such as Pluronic P123) and by adjusting the synthesis conditions.

EXPERIMENTAL SECTION

Experimental details on the chemicals used for synthesis of organosilica materials and characterization and calculations are provided in the Supporting Information.

Preparation of Materials. Mesoporous silica samples with diethylphosphatoethyl groups were prepared according to the slightly modified procedure reported for the synthesis of SBA-15.[32] In a typical synthesis, Pluronic P123 (2 g) was dissolved in 61.2 mL of 2 M HCl and 10.8 mL of deionized water at 40 °C during 3.5 h under rapid stirring. Next, 4.43 mL (0.02 mmol) of TEOS was added dropwise under stirring to the polymer solution at 40 °C. After half an hour, the specified amount of diethylphosphatoethyltriethoxysilane (DPTS; 20, 40%) was added to the synthesis gel, which was further stirred for 24 h and aged at 100 °C. The resulting template-containing organosilica was filtered and washed with 2 M HCl and dried overnight at 80 °C. The P123 template was extracted with 2 mL of 36% HCl and 100 mL of 95% of ethanol per gram of the sample at 70 °C for 24 h. Afterward, the mixture was transferred to a Petri dish and dried in an oven at 100 °C for 24 h. In total, 1 g of the extracted material was treated with concentrated HCl solution at 60 °C for 20 h in the reflux condenser to convert [$-P{=}O(OC_2H_5)_2$] to [$-P{=}(O)\ (OH)_2$] groups. Finally, the product was washed with deionized water. The resulting mesoporous silica samples with diethylphosphatoethyl (DP) groups are labeled as DPX, where X denotes the molar percentage of DPTS in the initial synthesis mixture: (X%) = [moles of DPTS × 100]/[moles of DPTS + moles of TEOS]. The amount of TEOS (0.02 mol) was the same in all syntheses. All extracted and as-synthesized samples are marked with an asterisk * and #, respectively. Conversion of DP groups in the DPX samples to hydroxyphosphatoethyl groups produces the DPX−OH samples. In other words, DPX*−OH refers to the samples with diethylphosphatoethyl groups extracted with HCl−ethanol solution (see above) and subjected to the treatment with concentrated HCl to convert [$-P{=}O(OC_2H_5)_2$] to [$-P{=}(O)\ (OH)_2$] groups. For instance, DP40*−OH denotes the sample prepared using 40% of DPTS, extracted, and reacted with concentrated HCl to obtain mesoporous silica with [$-P{=}(O)\ (OH)_2$] groups.

Equilibrium Adsorption Measurements for Lead Ions. Several solutions of heavy metal ion (Pb^{2+}) with different initial concentrations (50, 100, 150, 200, 250, 300 mg/L) were prepared to measure the equilibrium adsorption. A volume of 50 mL of each heavy metal ion solution with 0.01 g of the silica material (V/m = 5000) were placed under stirring (150 rpm, 22 °C, pH = 4.8) for 3 h. The amount of

DOI: 10.1021/acsami.5b06951
ACS Appl. Mater. Interfaces XXXX, XXX, XXX−XXX

adsorbed heavy metal ions per unit mass of the solid at equilibrium, (q_e), was determined as follows

$$q_e = \frac{(C_0 - C_e)V}{m} \quad (1)$$

where C_0 (mg/L) is the initial concentration of lead ions, V (mL) is the volume of lead ion solution, and m (g) is the mass of the adsorbent. C_e (mg/L) is the equilibrium concentration of Pb^{2+} determined by atomic adsorption spectroscopy (AAS-BUCK Scientific; model 210 VGP; Pb primary wavelength, 283.2 nm).

Kinetic Adsorption Experiments for Lead Ions. Kinetic adsorption measurements were performed using aqueous solution of lead ions with an initial concentration of 100 mg/L. In total, 0.01 g (V/m = 5000, V = 50 mL) of the modified silica material were placed under similar experimental conditions as those used in equilibrium measurements (150 rpm stirring, 22 °C, pH = 4.8). A volume of 0.5 mL of the initial solution was taken before mixing the adsorbent and lead ion solution (t = 0) and at predetermined time intervals (t = 10−120 min). The amount of adsorbed lead ions per unit mass of the adsorbent at time t, (q_t), was determined by the following equation:

$$q_t = \frac{(C_0 - C_t)V}{m} \quad (2)$$

where C_t (mg/L) is the concentration of lead ions at a given time, and other symbols have the same meaning as above.

Equilibrium Adsorption Data Analysis. The Langmuir isotherm equation is commonly used for analysis of equilibrium adsorption data. The Langmuir adsorption model is based on several assumptions such as all sites are identical and energetically equivalent, lateral interactions are neglected, and adsorption is limited to the formation of monolayer only (adsorption takes place on homogeneous sites and each site can accommodate only one metal ion).[33] On the basis of the Langmuir model, adsorption of lead ions on the silica substrate can be expressed as

$$q_e = K_L C_e q_m/(1 + K_L C_e) \quad (3)$$

where K_L is the Langmuir constant, C_e is the equilibrium concentration, q_m and q_e are the maximum and equilibrium adsorbed quantities, respectively. Equation 3 was fitted to the experimental adsorption data using nonlinear regression to obtain the values of K_L and q_m. Alternatively, the following linear form of Equation 3 can be used:

$$\frac{1}{q_e} = \frac{1}{q_m} + \frac{1}{K_L q_m}\frac{1}{C_e} \quad (4)$$

By plotting $1/q_e$ vs $1/C_e$, one can also calculate the aforementioned q_m and K_L parameters and validate the curve fitting by determining the R^2 correlation coefficient.

Models Used to Analyze Adsorption Kinetics Data. Analysis of adsorption kinetics data was performed by using the two most popular models. The first order adsorption kinetics model proposed by Lagergren[34] and developed by Krishnan:[35]

$$dq/dt = K_1(q_e - q_t) \quad (5)$$

where q_e and q_t are the amounts of adsorbed metal ions at the equilibrium and time t, respectively. K_1 is the rate constant of the first order adsorption reaction. Integration of the above equation gives

$$\log(q_e - q_t) = -K_1 t/2.303 + \log q_e \quad (6)$$

Plotting log ($q_e - q_t$) versus t can be used to find K_1. The pseudo-second order kinetic model reported by Ho and Mckay[36] can be presented in the following form:

$$dq/dt = K_2(q_e - q_t)^2 \quad (7)$$

where K_2 is the pseudo-second order rate constant (g mg^{-1} min^{-1}). The integrated linear form of the above equation can be presented as follows:

$$t/q_t = 1/(K_2 q_e^{\,2}) + t/q_e \quad (8)$$

K_2 and q_e can be easily determined from the slope and intercept of the t/q_e vs time plot.

RESULTS AND DISCUSSION

Properties of Diethylphosphatoethyl-Functionalized OMS Samples. The thermal stability of the diethylphosphatoethyl and hydroxyphosphatoethyl groups present in DP-MS and POH-MS was investigated by high-resolution thermogravimetry (TG). The TG and DTG (differential TG) profiles were used to study the thermal behavior of the as-synthesized (DP20#), extracted (DP20*), and acid-treated (DP20*−OH) DP20 samples. The DTG and TG curves recorded for these samples are presented in Figure 1 and Figure S2 in the

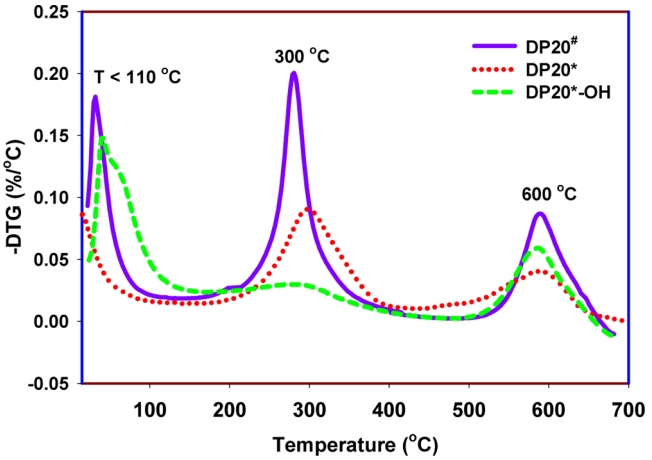

Figure 1. DTG curves for as-synthesized (#), extracted (*), and hydroxyphosphatoethyl functionalized DP20 samples.

Supporting Information, respectively. The DTG profile of DP20# shows three peaks: the first at 25−110 °C reflecting thermodesorption of physisorbed water, the second at about 300 °C represents the thermal decomposition of Pluronic P123, and the remaining peak at about 600 °C reflects the degradation of diethylphosphatoethyl groups. As in the case of DP20#, the DTG profile of DP20* exhibits also three analogous peaks at similar temperature ranges but the intensity of the second peak is much smaller due to the removal of Pluronic P123; however, the presence of this peak indicates that the extraction of P123 was incomplete. Finally, the lack of the second peak on the DTG profile of DP20*−OH (Figure 1) indicates that block copolymer was completely removed upon treatment of the extracted DP20* sample with concentrated HCl.

Small angle X-ray diffraction (XRD) was used to identify the mesostructural ordering of the organosilica samples studied. The XRD spectra of the extracted (DP20*) and hydroxyphosphatoethyl-modified (DP20*−OH) samples are presented in Figure 2. Both samples exhibit three peaks, one sharp at $2\theta \sim 0.85°$ and two minor peaks at $2\theta \sim 1.4°$ and 1.6°, respectively, which can be indexed as 100, 110, and 200 peaks characteristic for hexagonally ordered mesostructures (*p6mm* symmetry group). In fact, the TEM images of DP20* and DP20*−OH displayed in Figure 3 (left and right panels, respectively) reflect high mesostructural ordering of DP20* and further support the XRD results. However, the XRD spectra for the samples with a higher concentration of surface ligands

DOI: 10.1021/acsami.5b06951
ACS Appl. Mater. Interfaces XXXX, XXX, XXX−XXX

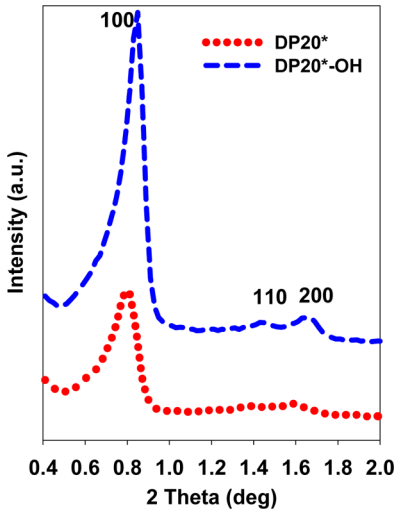

Figure 2. Small angle XRD spectra of the extracted (*) and hydroxyphosphatoethyl functionalized DP20 samples.

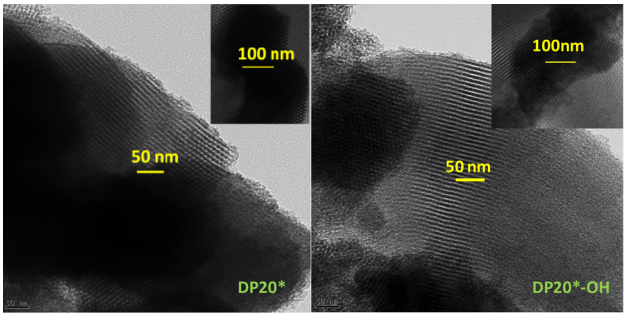

Figure 3. TM images of the DP20* (left panel) and DP20*−OH samples (right panel).

(DP40* and DP40*−OH) show only one broad peak in the 2θ range from about 0.4 to 1.0 suggesting uniform but rather disordered (not shown here).

Nitrogen adsorption−desorption isotherms collected for DP20*/DP20*−OH and DP40*/DP40*−OH samples at −196 °C are presented, respectively, in Figures 4 and S3 in Supporting Information (left panel). As can be seen from Figure 4 left panel, DP20* and DP20*−OH exhibit type IV isotherm with a H1 hysteresis loop starting at the relative pressure of about 0.65−0.75 and 0.55−0.65, respectively. A shift of the hysteresis loop of DP20*−OH toward lower pressures indicates a decrease in the size of mesopores as compared to that of DP20*. However, adsorption isotherms for DP40* and DP40*−OH are type IV with H2 hysteresis loop characteristic for cage-like and/or constricted mesopores. Thus, an increase in the loading of diethylphosphotoethyl groups in the mesostructure results in the deterioration of the mesostructural ordering. The specific surface area, the volume of fine pores (i.e., pores below 3 nm), the volume of primary mesopores, the mesopore diameter, and the single-point pore volume were evaluated using nitrogen adsorption isotherms measured at −196 °C (see Table 1). The PSD curves calculated for DP20* and DP20*−OH (Figure 4, right panel) are narrow and reflect the uniformity of mesopores;[37] however, bimodal PSD curves were obtained for DP40* and DP40*−OH samples (Figure S3, right panel). Moreover, the specific surface area, single-point pore volume, and the volume of fine pores decrease with increasing amount of diethylphosphatoethyl groups in the samples studied from DP20* to DP40*. For instance, the specific surface area changes from 448 for DP20* to 255 $m^2\ g^{-1}$ for DP40*, the pore volume changes from 0.59 for DP20* to 0.34 $cm^3\ g^{-1}$ for DP40*, and the volume of fine pores changes from 0.07 for DP20* to 0.04 $cm^3\ g^{-1}$ for DP40*.

As can be seen from Figures 4 and S3 (Supporting Information), the shape of adsorption isotherms and the corresponding PSD curves did not differ significantly for the DPX* and DPX*−OH (X = 20, 40) samples. Another exciting feature of the DPX*−OH mesostructures is an enhancement in the surface properties due to the conversion of DP groups. This is possibly due to the removal of the remaining part of P123 block copolymer from the noncompletely extracted sample (compare DTG curves for DP20* and DP20*−OH in Figure 1 at 300 °C). For instance, the BET surface area changes from 448 for DP20* to 576 $m^2\ g^{-1}$ for DP20*−OH, the single-point pore volume changes from 0.59 for DP20* to 0.65 $cm^3\ g^{-1}$ for DP20*−OH, and the volume of fine pores changes from 0.07 for DP20* to 0.10 $cm^3\ g^{-1}$ for DP20*−OH. However, the pore diameter decreases from 8.0 for DP20* to 7.6 nm for DP20*−OH (see Table 1). Similar change in the aforementioned surface properties can also be observed for the DP40* and DP40*−OH samples.

Table 1. Structural Parameters of the DPX* and DPX*−OH (X = 20,40) Samples Studied[a]

content	V_{sp} (cc/g)	V_{mic} (cc/g)	S_{BET} (m^2/g)	W_{max} (nm)	V_t (cc/g)
DP20*	0.59	0.07	448	8.0	0.64
DP40*	0.34	0.04	255	5.7	0.35
DP20*−OH	0.65	0.10	576	7.6	0.68
DP40*−OH	0.39	0.06	325	5.4	0.40

[a] V_{sp}, single point pore volume calculated at the relative pressure of 0.98; V_{mic}, volume of fine pores (micropores and small mesopores below 3 nm) calculated by integration of the PSD curve up to 3 nm; S_{BET}, specific surface area calculated from adsorption data in relative pressure range 0.05−0.20; W_{max}, pore width calculated at the maximum of PSD, using improved KJS method; V_t, total pore volume calculated by integration of the PSD curve.

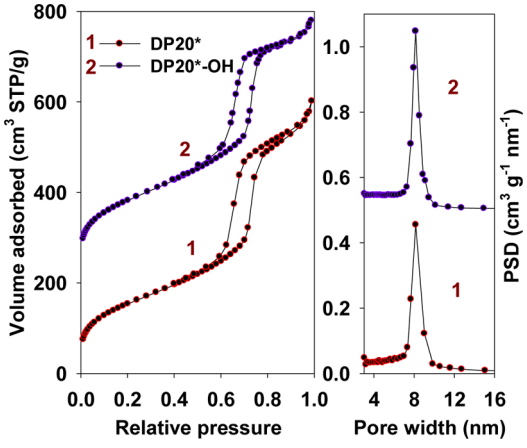

Figure 4. Nitrogen adsorption isotherms (left panel) and the corresponding PSD curves (right panel) for extracted (*) and hydroxyphosphatoethyl functionalized DP20 samples; the second isotherm is shifted by 300 cm^3 STP/g in relation to curve 1. The PSD curve 2 is shifted by 0.54 $cm^3\ g^{-1}\ nm^{-1}$ in relation to curve 1.

DOI: 10.1021/acsami.5b06951
ACS Appl. Mater. Interfaces XXXX, XXX, XXX−XXX

$^{1}H-^{13}C$ CP/MAS NMR spectra and ^{31}P single pulse NMR spectra were used to verify the existence of diethylphosphatoethyl groups in the mesostructures studied. The $^{1}H-^{13}C$ cross-polarization (CP)-MAS NMR spectra were recorded for the DPTS, DP20*, and DP20*−OH samples (Figure 5). The

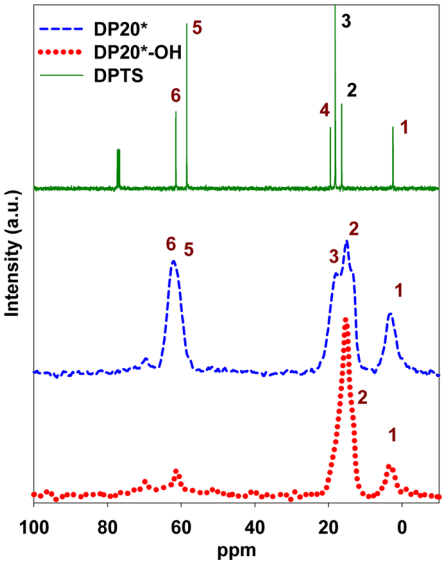

Figure 5. $^{1}H-^{13}C$-CP/MAS NMR spectra of diethylphosphatoethyltriethoxysilane (DPTS), DP20*, and DP20*−OH samples.

spectrum recorded for DPTS silane exhibits five peaks at chemical shifts 2.5, 16.4, 18.2, 19.5, 58.5, 61.4 ppm, which can be assigned to the methylene carbon atom directly bonded to silicon ($-Si-(C)H_2-CH_2-P-$), to the methylene carbon atom linked to phosphorus ($-Si-CH_2-(C)H_2-P-$), to the methyl carbon of two ethoxy groups in $PO(O-CH_2-(C)H_3)$, to the methyl carbon atoms of nonhydrolyzed ethoxy group in ($-Si-O-CH_2-(C)H_3$-), methylene carbon atoms in the nonhydrolyzed ethoxy groups ($-Si-O-(C)H_2-CH_3$-), and, finally to the methylene carbon atoms in the ethoxy group in $PO(O-(C)H_2-(C)H_3)$ (compare Figures 5 and 6).[12−14,38−41]

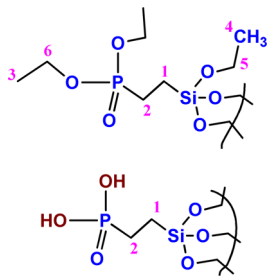

Figure 6. Systematic illustration of surface groups used for assignment of ^{13}C-CP/MAS NMR spectra peaks.

The DP20* sample shows chemical shifts at 3.1, 15.3, 18.2, and 60.5, which correspond to the methylene carbon atoms bonded to silicon, methylene carbon atoms connected to phosphorus, methyl carbon of two ethoxy groups in $PO(O-CH_2-(C)H_3)$, and methylene carbon atoms of the ethoxy groups in $PO(O-(C)H_2-(C)H_3)$.[12−14,38−41] The unreacted (nonhydrolyzed) $-Si-O-CH_2-(C)H_3-$ can also be present even after the synthesis is completed. Thus, the overlapping of 15.3 and 18 ppm signals may mask the methyl carbon species of the nonhydrolyzed ethoxy group in ($-Si-O-CH_2-(C)H_3-$), while the 58.5 ppm peak can be masked by that corresponding to methylene carbon atoms of the ethoxy group in $PO(O-(C)H_2-(C)H_3)$. After 24 h acidic treatment, the DP20*−OH sample shows two broad lines attributed to the methylene carbon atom bonded to silicon ($-Si-(C)H_2-CH_2-P-$) and phosphorus ($-Si-CH_2-(C)H_2-P-$).[12−14,38−41] The disappearance of the ethyl group ($-C_2H_5$) in $PO(O-C_2H_5)$ and $Si-OC_2H_5$ is due to the concentrated HCl treatment.

^{31}P single pulse NMR spectra were also recorded for the DPTS, DP20*, and DP20*−OH samples (see Figure 7). These

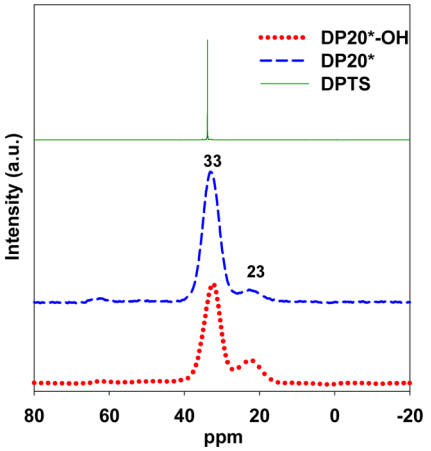

Figure 7. $^{1}H-^{31}P$ CP-MAS NMR spectra of diethylphosphatoethyltriethoxysilane, DP20*, and DP20*−OH samples.

spectra display only one major signal at 33 ppm indicating a homogeneous environment of phosphorus in the phosphonate ($-P=O-C_2H_5$) group. However, the DP20* sample shows two chemical shifts at δ = 33 and 23 ppm (δ = chemical shift scale), which can be indicative of forming two distinct phosphorus environments, surface interactions between phosphrous in phosphonic acid and the framework. The peaks at δ = 33 and 23 ppm can be assigned to hydrogen bond acceptor and donor, respectively.[12−14,38−41] According to the literature, phosphonic acid group acts as a hydrogen bond donor via P−OH groups and hydrogen bond acceptor via the P=O bond. Acceptance of electron changes the strength electron density around the P atom and the ^{31}P nucleus become unshielded, which results in shifting phosphorus resonance to a lower chemical shift at δ = 23 ppm. The DP20*−OH sample also shows a P^{31} NMR pattern similar to that of DP20*. However, the peak intensity at 23 ppm is higher than that of DP20*, which further indicates the enhancement of electron density around the P atom. The $^{1}H-^{29}Si$ CP/MAS NMR spectrum of DP20* exhibits two peaks (Figure 8) at −68.3 and −101.6 ppm that can be assigned to $T^3[R-Si-(OSi)_3]$ and T^3/Q^4 $[Si-(OSi)_3(OH)/Si-(OSi)_4]$ groups, respectively. The spectrum of DP20*−OH also displays peaks at −67.7 and −101.7 ppm attributed to the $T^3[R-Si-(OSi)_3]$ and T^3/Q^4 $[Si-(OSi)_3(OH)/Si-(OSi)_4]$ groups, respectively. The peak at 110.5 ppm visible for both DP20* and DP20*−OH samples can be assigned Q^4 $[Si-(OSi)_4]$ groups. Note that peak positions of DP20*−OH does not show any significant deviation (ppm) in comparison to that of DP20*−OH. This finding confirmed the stability of siloxane bonds during the conversion of DP20* to DP20*−OH.

DOI: 10.1021/acsami.5b06951
ACS Appl. Mater. Interfaces XXXX, XXX, XXX−XXX

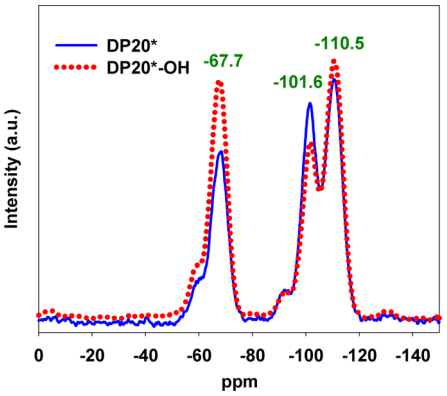

Figure 8. $^{1}H-^{29}Si$-MAS NMR spectra of the DP20* and DP20*−OH samples.

Lead (Pb^{2+}) Adsorption and Possible Interactions with Hydroxylphosphatoethyl Groups. Kinetic study of the adsorption process is important because it provides valuable information about the rate of Pb^{2+} uptake by the DPX* and DPX*−OH samples, reaction pathways, and possible binding mechanism. Figure 9 shows the time dependence of adsorption

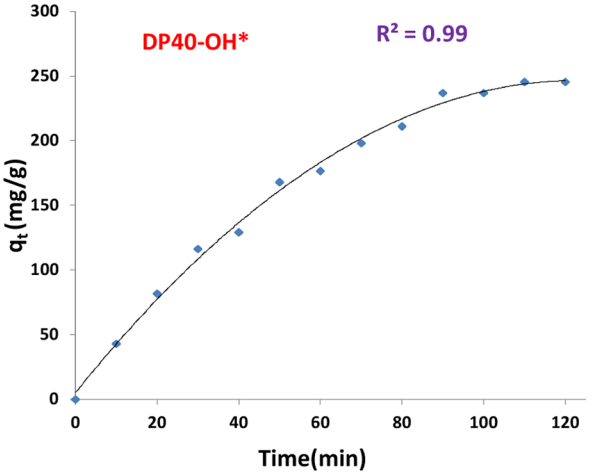

Figure 9. Experimental adsorption kinetics of Pb^{2+} ions on the selected CP40*−OH sample.

of Pb^{2+} ions on DP40*−OH. The linear forms of the pseudo-first-order and pseudo-second-order kinetics equations were used to plot the experimental data as described in the Experimental Section. Equations 6 and 8, being linear forms of eqs 5 and 7, respectively, were used to check the validity of these equations and to determine their parameters. As can be seen in Figures S4 (Supporting Information) and Figure 10, the correlation coefficient values (R^2) for the pseudo-first-order and second-order kinetics models exceeded 0.90 and 0.97, respectively. Thus, the lead uptake is well fitted by the pseudo-second-order kinetics model indicating that this model better represents the experimental data of Pb^{2+} sorption.

Sorption capacities for DP20*, DP40*, DP20*−OH, and DP40*−OH were obtained by measuring sorption data for a series of Pb^{2+} concentrations in the range of 50 to 300 (mg/L). The Pb^{2+} adsorption isotherms represent the amount of lead adsorbed at equilibrium (q_e) as a function of the equilibrium Pb^{2+} concentration, C_e, (mg L^{-1}) at pH = 4.8 at 22.0 °C for the samples studied. These isotherms are shown in Figure 11 and

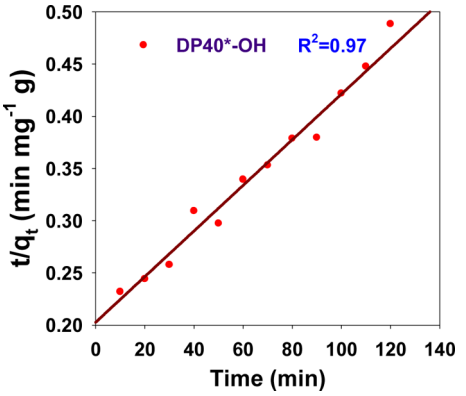

Figure 10. Linear form of adsorption kinetics equation for pseudo second-order model for Pb^{2+} adsorption on the DP40*−OH.[36]

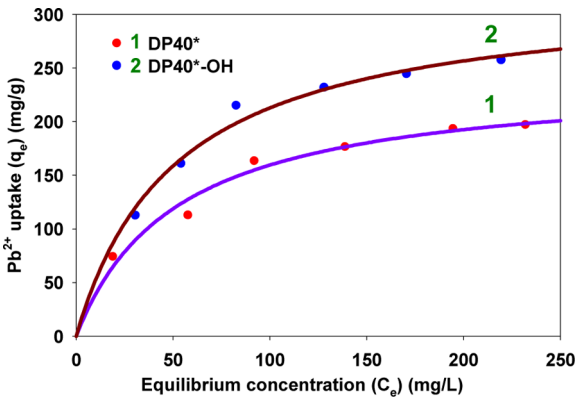

Figure 11. Experimental Pb^{2+} adsorption isotherms at 22 °C and nonlinear regression Langmuir curves for DP40* and DP40*−OH.

Figure S5 in the Supporting Information. These figures show that adsorption of Pb^{2+} initially increase with increasing lead concentration and then levels off. The high Pb^{2+} uptake at the beginning of the equilibrium isotherm may be caused by the availability of many chelating diethylphosphatoethyl and hydroxyphosphatoethyl groups, which are essential for attracting these ions from solution. The experimental data were correlated by the nonlinear form of Langmuir eq 3 and its parameters (q_m and K_L) were calculated by curve fitting and listed in Table 2. High correlation coefficients (R^2), larger than

Table 2. Langmuir Model Parameters Calculated for the DPX* and DPX*−OH (X = 20,40) Samples Studied[a]

content	q_m	std error	K_L	std error	R^2
DP20*	116	5.87	0.016	0.001	0.96
DP40*	202	5.01	0.024	0.003	0.97
DP20*−OH	168	2.15	0.019	0.002	0.96
DP40*−OH	272	4.87	0.029	0.004	0.97

[a] q_m, maximum Pb^{2+} adsorption capacity expressed in mg/g, and Langmuir constant evaluated according to eq 4 in which concentration is expressed in mg/L.

0.96, indicate the usefulness of the Langmuir model for analysis of lead adsorption on the CP20*, CP40*, CP20*−OH, and CP40*−OH samples studied. The linear form of Langmuir eq 4 was also used to validate the curve fitting (R^2) values. These isotherms are shown in Figures S6 and S7 in the Supporting Information.

DOI: 10.1021/acsami.5b06951
ACS Appl. Mater. Interfaces XXXX, XXX, XXX−XXX

Lead (Pb^{2+}) ion uptakes measured for all DPX* and DPX*−OH (X = 20, 40) samples are listed in Table 2, which shows that the lead ion uptake for DP40* (202 mg/g) is amazingly competitive as compared to the corresponding value obtained for DP20* (116 mg/g) sample. DP40* adsorbed two times more lead ions as compared to adsorption on DP20*. An average Langmuir constant value for DP40* is higher than that of DP20* due to the higher concentration of bonded ligands in the former sample. A successful conversion of diethylphosphatoethyl (DPX*; X = 20, 40) groups to hydroxyphosphatoethyl functionalities (DPX*−OH; X = 20, 40) results in an increase of the chelating ability of the latter group toward lead ions.

For instance, DP40*−OH shows higher lead ions uptake (272 mg/g) than that of DP40* (see the uptakes obtained for the DP40*−OH and DP40* samples listed in Table 2). Naturally, DPX*−OH exhibits more metal chelating groups having −OH and O− than the corresponding parent DPX* samples. Concentration of bonded ligands plays a very important role in adsorption. Thus, the loading of bonded ligands was optimized by increasing the molar percentage of DPTS with respect to TEOS up to 60%. However, it was shown that an increase in the percentage of DPTS in the reaction mixture over 40% (samples DP50* and DP60*) led to a pronounced change in the N_2 adsorption−desorption isotherms, indicating that the surface properties of the resulting mesoporous organosilicas are dependent on the loading of organic groups. A significant deterioration in the mesostructural ordering was observed at high loadings (50 and 60%) of diethylphosphatoethyl groups. The volumes of adsorbed nitrogen on DP50* and DP60* are much smaller, indicating a substantial reduction in the surface area and total pore volume. For instance, the specific surface area dropped from 255 m^2/g for DP40* to 87 and 33 m^2/g for DP50* and DP60*, respectively. Similarly, the total pore volume dropped from 0.35 cm^3/g for DP40* to 0.24 and 0.09 cm^3/g for DP50* and DP60*, respectively. Also, a significant shift in direction of low pressures was observed in the capillary condensation steps, indicating much smaller pore sizes. The observed decrease in the aforementioned adsorption parameters is expected due to the high loading of diethylphosphatoethyl groups into the mesostructure, which occupy some portion of pores and cause a significant reduction in the pore size, pore volume, and surface area of the organosilica studied. Consequently, Pb^{2+} uptakes measured for both DP50* and DP60* samples are below 150 mg/g. This may be due to inaccessibility of diethylphosphatoethyl groups for proper coordination of Pb^{2+} ions. Therefore, the subsequent conversion of DP50* and DP60* to DP50*−OH and DP60*−OH was not performed. A significant deterioration of the adsorption properties of DP50* and DP60* in comparison to DP40* suggests that the latter sample has an optimal loading of organic groups for adsorption of lead ions.

In order to show adsorption of Pb^{2+} on the selected mesoporous silica samples with hydroxyphosphatoethyl functionalities, the EDX spectra were recorded for DP20*−OH before and after adsorption of lead ions (see Figures S8 and S9 in the Supporting Information). The EDX spectrum of DP20*−OH after Pb^{2+} adsorption shows the presence of the lead peak, which is a clear indication of the chelation of lead ions by P−OH-containing groups. Nevertheless, it is somewhat difficult to understand the binding mechanism between Pb^{2+} ions and $[-P{=}O(OC_2H_5)_2]$ and $[-P{=}(O)\ (OH)_2]$chelating ligands. As described in the Introduction, lone pairs of oxygen atoms, which usually donate electrons to electron deficient Pb^{2+} ions, form a stable complex. It is obvious that the chelating ability of $(-OC_2H_5)$, hydroxyl (−OH), and deprotonated hydroxyl $(-O^-)$ groups increases according to the following order: $(-OC_2H_5) < (-OH) < (-O^-)$. Thus, at least one deprotonated hydroxyl group presents in DPX*−OH can effectively bind Pb^{2+}. Therefore, high sorption capacity obtained for DPX−OH materials make them potential sorbents for removal of lead ions from contaminated water. On the basis of the Pearson HSAB theory, the large electronegativity differences between a moderately hard acid such as Pb^{2+} and hard bases $(O^-)/(OH)$ give rise to strong ionic interactions (Figure 12). The complex formation shown in Figure 12 is a reasonable mechanism to explain interactions between Pb^{2+} and $[-P{=}O(OC_2H_5)_2]$ and $[-P{=}(O)\ (OH)_2]$ functionalities.

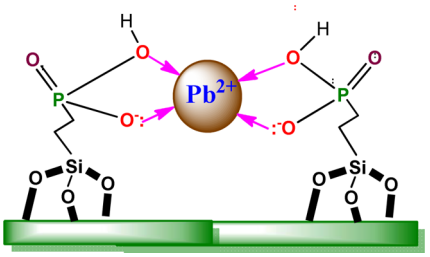

Figure 12. Systematic illustration of Pb^{2+} binding with hydroxyphosphatoethyl-group present in the siliceous mesostructure.

Many papers have been published on the removal of heavy metal ions by using mesoporous silica modified with various ligands such as mercaptopropyl, thiourea, thioether, aminopropyl, phenyls, vinyl, and carboxylic acid. The current study reports a two-step preparation of the silica-based adsorbents involving (i) Pluronic P123-assisted co-condensation synthesis of diethylphosphatoethyl-containing mesoporous silica (DP-MS) by using diethylphosphatoethyltriethoxysilane (DPTS) and (ii) conversion of diethylphosphatoethyl groups into hydroxyphosphatoethyl groups by using concentrated hydrochloric acid. Usually, the grafting of mesoporous silica supports is performed by introducing various ligands such as mercaptopropyl, thiourea, thioether, aminopropyl, phenyl vinyl, and carboxylic acid but their affinity and selectivity toward lead ions in acidic medium is relatively small. Note that in contrast to the aforementioned ligands, the diethylphosphatoethyl and hydroxyphosphatoethyl groups are highly selective for lead ions as compared to other metal ions such as Cu^{2+}, Hg^{2+}, Ag^+, Cu^{2+}, Ni^{2+}, and Cr^{3+}. Only this specific selectivity is reduced in the presence of uranium species at high concentrations. On the other side, hydroxyphosphatoethyl is a new type of bidentate ligand for lead adsorption as compared to the aforementioned monodentate ligands; usually bidentate ligands have higher chelating power than monodentate ones. For instance, four mercaptopropyl ligands in proper proximity are needed to provide proper coordination for lead ions, whereas only two diethylphosphatoethyl groups are sufficient to provide similar coordination chemistry. Moreover binding chemistry of lead ions with $P{=}(O)\ (OH)_2$ or $-P{=}(O)(O-)\ (OH)$ leads to high Pb^{2+} uptake as compared to the previously reported publications. For instance, Tang and co-workers used (3-glycidyloxypropyl)trimethoxysilane (GLYMO) and iminodiacetic acid (IDA) to prepare GLYMO-IDA silane for lead removal at highly acidic pH

DOI: 10.1021/acsami.5b06951
ACS Appl. Mater. Interfaces XXXX, XXX, XXX−XXX

(~2) and mild acidic pH (~4.5) conditions.[42] A tridentate −N and −COOH functionalized GLYMO-IDA materials adsorbed 103 mg/g and 160 mg/g of Pb^{2+} ions, respectively, at pH = 2 and 4.5. A novel acid−base bifunctional siliceous adsorbent was synthesized by Yu and co-workers and applied for removal of lead ions at pH = 5.0;[43] the highest uptake of lead ions by this sorbent was about 147.5 mg/g. Thiol-functionalized MCM-41 mesoporous silica materials used by Li and co-workers[44] to remove Pb^{2+} ions adsorbed only about 66.04 mg/g. The core−shell magnetic mesoporous microspheres with amino groups developed for removal of Pb(II) and Cd(II) ions by Wang and co-workers adsorbed 128.2 and 51.8 mg/g of Pb^{2+} and Cd^{2+}, respectively.[45] Large pore diameter MCM-41 was also used to remove lead ions from aqueous media by Gibson and co-workers; they reported the maximum lead uptake of about 207 mg/g.[46] In all these cases the adsorption capacity values reported for Pb^{2+} ions were smaller than that measured for our material, DP40*−OH.

Recovery of Pb^{2+} ions from adsorbent is also an important step. Thus, the sorbents were washed with 0.01, 0.1, or 1.0 M HCl aqueous solutions to investigate Pb^{2+} removal and determine the affinity of the diethylphosphatoethyl and hydroxylphosphatoethyl ligands toward Pb^{2+} ions. Analysis of the supernatant obtained by washing the sample with 0.01 M HCl indicates that the sorbent has a strong affinity toward Pb^{2+} ions because Pb^{2+} ions were not removed. After washing with 0.1 M HCl, the amount of lead ions remaining in the sorbent was about 40−60%. However, more than 99% of Pb^{2+} was removed from diethylphosphatoethyl and hydroxylphosphatoethyl functionalized surfaces after washing with 1 M HCl. Thus, these materials can be repeatedly used for Pb^{2+} adsorption after treatment with 1 M HCl.

CONCLUSIONS

A series of diethylphosphatoethyl and hydroxyphosphatoethyl-functionalized mesoporous silica materials was studied as prospective adsorbents for lead ions from aqueous solutions. ^{13}C and ^{31}P NMR spectra confirmed straightforwardly and unequivocally the aforementioned functionalization of siliceous mesostructures. The resulting materials exhibited a relatively high surface area (close to 600 m^2/g) and accessible mesopores of about 7.6 nm in diameter. The proposed functionalization of mesoporous silica such as SBA-15 by covalent bonding of multifunctional P-containing ligands afforded highly effective materials for adsorption of lead ions from polluted water. These materials showed high affinity to coordinate lead ions effectively at both low and high concentrations. Adsorption isotherms measured for lead ions on DP-MS and POH-MS can be well fitted by the Langmuir equation. The highest adsorption capacities, 272 and 168 mg of lead ions per gram of the adsorbent, were obtained for the DP40*−OH and DP20*−OH samples, respectively. It is evident that the presence of hydroxyphosphatoethyl groups in the DP20*−OH mesostructure, able to effectively chelate lead ions, led to a substantial enlargement of the adsorption capacity of this organosilica as compared to that with diethylphosphatoethyl surface groups. It is shown that high loading of diethylphosphotoethyl and hydroxyphosphotoethyl groups in the organosilica mesostructures studied can be achieved by using one-pot co-condensation synthesis, which is much more effective for lead adsorption than postsynthesis grafting. Large adsorption capacity, high selectivity, low cost of preparation of the materials studied together with good chemical and thermal stability of the introduced groups prove their potential for the treatment of Pb^{2+}contaminated water.

ASSOCIATED CONTENT

Supporting Information

The Supporting Information is available free of charge on the ACS Publications website at DOI: 10.1021/acsami.5b06951.

Scheme illustrating the conversion of DP-MS to the POH-MS and eight figures with TG curves, nitrogen adsorption isotherms, linear plot of adsorption kinetics, nonlinear plot of adsorption isotherms, two linear regression plots, and two EDX spectra for the samples studied (PDF)

AUTHOR INFORMATION

Corresponding Author

*E-mail: jaroniec@kent.edu.

Notes

The authors declare no competing financial interest.

ACKNOWLEDGMENTS

The TEM data were obtained at the (cryo) TEM facility at the Liquid Crystal Institute, Kent State University, supported by the Ohio Research Scholars Program Research Cluster on Surfaces in Advanced Materials. The authors thank Dr. Min Gao and Michal Marszewski for technical support with the TEM experiments. Thanks to Dr. Mahinda Gangoda for technical support with the NMR measurements.

REFERENCES

(1) Feng, X.; Fryxell, G. E.; Wang, L.-Q.; Kim, A. Y.; Liu, J.; Kemner, K. M. Functionalized Monolayers on Ordered Mesoporous Supports. *Science* **1997**, *276*, 923−926.

(2) Wu, H. Y.; Chen, C. T.; Hung, I. M.; Liao, C. H.; Vetrivel, S.; Kao, H. M. Direct Synthesis of Cubic Benzene-Bridged Mesoporous Organosilica Functionalized with Mercaptopropyl Groups as an Effective Adsorbent for Mercury and Silver Ions. *J. Phys. Chem. C* **2010**, *114*, 7021−7029.

(3) Antochshuk, V.; Olkhovyk, O.; Jaroniec, M.; Park, I. S.; Ryoo, R. Benzoylthiourea-Modified Mesoporous Silica for Mercury(II) Removal. *Langmuir* **2003**, *19*, 3031−3034.

(4) Liu, A. M.; Hidajat, K.; Kawi, S.; Zhao, D. Y. A New Class of Hybrid Mesoporous Materials with Functionalized Organic Monolayers for Selective Adsorption of Heavy Metal Ions. *Chem. Commun.* **2000**, 1145−1146.

(5) Zhang, L. X.; Zhang, W. H.; Shi, J. L.; Hua, Z.; Li, Y. S.; Yan, J. A New Thioether Functionalized Organic−Inorganic Mesoporous Composite as a Highly Selective and Capacious Hg^{2+} Adsorbent. *Chem. Commun.* **2003**, 210−211.

(6) Benitez, M.; Das, D.; Ferreira, R.; Pischel, U.; Garcıa, H. Urea-Containing Mesoporous Silica for the Adsorption of Fe(III) Cations. *Chem. Mater.* **2006**, *18*, 5597−5603.

(7) Wu, S.; Li, F.; Xu, R.; Wei, R.; Li, G. Synthesis of Thiol-Functionalized MCM-41 Mesoporous Silicas and its Application in Cu(II), Pb(II), Ag(I), and Cr(III) Removal. *J. Nanopart. Res.* **2010**, *12*, 2111−2124.

(8) Algarra, M.; Jimenez, M. V.; Castellon, E. R.; Lopez, A. J.; Jimenez, J. J. Heavy Metals Removal from Electroplating Wastewater by Aminopropyl-Si MCM-41. *Chemosphere* **2005**, *59*, 779−786.

(9) Denizli, A.; Say, R.; Patır, S.; Arıca, Y. M. Adsorption of Heavy Metal Ions onto Ethylene Diamine-Derived and Cibacron Blue F3GA-Incorporated Microporous poly(2-hydroxyethyl methacrylate) Membranes. *React. Funct. Polym.* **2000**, *43*, 17−24.

(10) Heidari, A.; Younesi, H.; Mehraban, Z. Removal of Ni(II), Cd(II), and Pb(II) from a Ternary Aqueous Solution by Amino

DOI: 10.1021/acsami.5b06951
ACS Appl. Mater. Interfaces XXXX, XXX, XXX−XXX

Functionalized Mesoporous and Nano Mesoporous Silica. *Chem. Eng. J.* **2009**, *153*, 70−79.
(11) Bala, T.; Prasad, B. L.; Sastry, M.; Kahaly, M. U.; Waghmare, A. U.V. Interaction of Different Metal Ions with Carboxylic Acid Group: A Quantitative Study. *J. Phys. Chem. A* **2007**, *111*, 6183−6190.
(12) Lebed, P. J.; Souza, K. D.; Bilodeau, F.; Lariviere, D.; Kleitz, F. Phosphonate- Functionalized Large Pore 3-D Cubic Mesoporous (KIT-6) Hybrid as Highly Efficien Actinide Extracting Agent. *Chem. Commun.* **2011**, *47*, 11525.
(13) Lebed, P. J.; Savoie, J. D.; Florek, J.; Bilodeau, F.; Larivière, D.; Kleitz, F. Large Pore Mesostructured Organosilica-Phosphonate Hybrids as Highly Efficient and Regenerable Sorbents for Uranium Sequestration. *Chem. Mater.* **2012**, *24*, 4166−4176.
(14) Yuan, L. Y.; Liu, Y. L.; Shi, W. Q.; Lv, Y. L.; Lan, J. H.; Zhao, Y. L.; Chai, Z. F. High Performance of Phosphonate-Functionalized Mesoporous Silica for U(VI) Sorption from Aqueous Solution. *Dalton Trans.* **2011**, *40*, 7446−7453.
(15) Wang, X. L.; Yuan, L. Y.; Wang, Y. F.; Li, Z. J.; Lan, J. H.; Liu, Y. L.; Feng, Y. X.; Zhao, Y. L.; Chai, Z. F.; Shi, W. Q. Mesoporous Silica SBA-15 Functionalized with Phosphonate and Amino Groups for Uranium Uptake. *Sci. China: Chem.* **2012**, *55*, 1705−1711.
(16) Dabrowski, A.; Barchak, M.; Dudarko, O. A.; Zub, Y. L. Preparation and Characterisation of Polysiloxane Xerogels Having Covalently Attached Phosphonic Asids Groups. *Polym. Chem. J.* **2007**, *81*, 475−483.
(17) Dudarko, O. A.; Goncharik, V. P.; Semenii, V. Y.; Zub, Y. L. Sorption of Hg^{2+}, Nd^{3+}, Dy^{3+}, and UO_2^{2+} ions at Polysiloxanexerogels Functionalized with Phosphonic Acid Derivatives. *Prot. Met.* **2008**, *44*, 193−197.
(18) Zhao, D.; Huo, Q.; Feng, J. Nonionic Triblock and Star Diblock Copolymer and Oligomeric Surfactant Syntheses of Highly Ordered, Hydrothermally Stable, Mesoporous Silica Structures. *J. Am. Chem. Soc.* **1998**, *120*, 6024−6036.
(19) Colilla, M.; Balas, F.; Manzano, M.; Manzano, M.; Regí, M. V. Novel Method to Enlarge the Surface Area of SBA-15. *Chem. Mater.* **2007**, *19*, 3099−3101.
(20) Kruk, M.; Jaroniec, M. Gas Adsorption Characterization of Ordered Organic-Inorganic Nanocomposite Materials. *Chem. Mater.* **2001**, *13*, 3169−3183.
(21) Wang, W.; Shan, W.; Ru, H. Facile Preparation and New Formation Mechanism of Plugged SBA-15 Silicas Based on Cheap Sodium Silicate. *J. Mater. Chem.* **2011**, *21*, 17433−17440.
(22) Pan, Y. C.; Tsai, H. H. G.; Jiang, J. C.; Kao, C. C.; Sung, T. L.; Chiu, P. J.; Saikia, D.; Chang, J. H.; Kao, H. M. Probing the Nature and Local Structure of Phosphonic Acid Groups Functionalized in Mesoporous Silica SBA-15. *J. Phys. Chem. C* **2012**, *116*, 1658−1669.
(23) Dudarko, O. A.; Zub, Y. L.; Barczak, M.; Dabrowski, A. Template Synthesis of Mesoporous Silicas Containing Phosphonic Groups. *Glass Phys. Chem.* **2011**, *37*, 596−602.
(24) Dudarko, O. A.; Gunathilake, C.; Sliesarenko, V. V.; Zub, Y. L.; Jaroniec, M. Microwave- Assisted and Conventional Hydrothermal Synthesis of Ordered Mesoporous Silicas with P- Containing Functionalities. Colloids and Surfaces A. *Colloids Surf., A* **2014**, *459*, 4−10.
(25) Puziy, A. M.; Poddubnaya, O. I.; Zaitsev, V. N.; Konoplitska, O. P. Modeling of Heavy Metal Ion Binding by Phosphoric Acid Activated Carbon. *Appl. Surf. Sci.* **2004**, *221*, 421−429.
(26) Freitas, O. M. M.; Martins, R. J. E.; Delerue-Matos, C. M.; Boaventura, R. A. R. Removal of Cd(II), Zn(II) and Pb(II) Fromaqueous Solutions by Brownmarine Macro Algae: Kinetic Modelling. *J. Hazard. Mater.* **2008**, *153*, 493−501.
(27) Paulino, A. T.; Santos, L. B.; Nozaki, J. Removal of Pb^{2+}, Cu^{2+}, and Fe^{3+} from Battery Manufacture Wastewater by Chitosan Produced from Silkworm Chrysalides. *React. Funct. Polym.* **2008**, *68*, 634−642.
(28) Jain, C. K.; Singhal, D. C.; Sharma, M. K. Adsorption of Zinc on Bed Sediment of River Hindon: Adsorption Models and Kinetics. *J. Hazard. Mater.* **2004**, *114*, 231−239.
(29) Sekar, M.; Sakthi, V.; Rengaraj, S. Kinetics Equilibrium Adsorption Study of Lead(II) onto Activated Carbon Prepared from Coconut Shell. *J. Colloid Interface Sci.* **2004**, *279*, 307−313.
(30) Iqbal, M.; Saeed, A.; Zafar, S. I. Hybrid Biosorbent: An Innovative Matrix to Enhance the Biosorption of Cd(II) from Aqueous Solution. *J. Hazard. Mater.* **2007**, *148*, 47−55.
(31) Corriu, R. J. P.; Datas, L.; Guari, Y.; Mehdi, A.; Reye, C.; Thieuleux, C. Ordered SBA−15 Mesoporous Silica Containing Phosphonic Acid Groups Prepared by a Direct Synthetic approach. *Chem. Commun.* **2001**, *8*, 763−764.
(32) Zhao, D.; Huo, Q.; Feng, J.; Chmelka, B. F.; Stucky, G. D. Nonionic Triblock and Star Diblock Copolymer and Oligomeric Surfactant Syntheses of Highly Ordered, Hydrothermally Stable, Mesoporous Silica Structures. *J. Am. Chem. Soc.* **1998**, *120*, 6024−6036.
(33) Sari, A.; Tuzen, M. Kinetic and Equilibrium Studies of Biosorption of Pb(II) and Cd(II) from Aqueous Solution by Macrofungus (Amanita rubescens) biomass. *J. Hazard. Mater.* **2009**, *164*, 1004−1011.
(34) Lagergren, S. Theorie Der Sogenannten Adsorption Gelöster Sstoffe. Kungliga Svenska Vetenskapsakademiens. *Handlingar* **1898**, *24*, 1−39.
(35) Annadurai, G.; Krishnan, M. R. V. Adsorption of Basic Dyes using Chitin. *Ind. J. Environ. Protect.* **1996**, *16*, 444−448.
(36) Ho, Y.; McKay, G. Pseudo-Second Order Model for Sorption Processes. *Process Biochem.* **1999**, *34*, 451−465.
(37) Kruk, M.; Jaroniec, M.; Sayari, A. Application of Large Pore MCM-41 Molecular Sieves to Improve Pore Size Analysis using Nitrogen Adsorption Measurements. *Langmuir* **1997**, *13*, 6267−6273.
(38) Aliev, A.; Ou, D. L.; Ormsby, B.; Sullivan, A. C. Porous Silica and Polysilsesquioxane with Covalently Linked Phosphonates and Phosphonic Acids. *J. Mater. Chem.* **2000**, *10*, 2758−2764.
(39) Bibent, N.; Charpentier, T.; Vinot, S. D.; Mehdi, A.; Gaveau, P.; Henn, F.; Silly, G. Solid- State NMR Spectroscopic Studies of Propylphosphonic Acid Functionalized SBA-15 Mesoporous Silica: Characterization of Hydrogen-Bonding Interactions. *Eur. J. Inorg. Chem.* **2013**, *13*, 2350−2361.
(40) Schrotter, J. C.; Cardenas, A.; Smaithi, M.; Hovnanian, N. Silicon and Phosphorus Alkoxide Mixture: Sol-Gel Study by Spectroscopic Techniques. *J. Sol-Gel Sci. Technol.* **1995**, *4*, 195−204.
(41) Melanic, I. V.; Stolyarchuk, N. V.; Dudarko, O. A.; Zub, Yu. L.; Dabrowski, A.; Barczak, M.; Alonso, B. Bridged Polysilsequioxane Adsorption Materials Containing Phosphonic Acid Residues. *Prot. Met. Phys. Chem. Surf.* **2010**, *46*, 206−214.
(42) He, R.; Li, W.; Deng, D.; Chen, W.; Li, H.; Wei, C.; Tang, Y. Efficient Removal of Lead from Highly Acidic Wastewater by Periodic Ion Imprinted Mesoporous SBA-15 Organosilica Combining Metal Coordination and Co-Condensation. *J. Mater. Chem. A* **2015**, *3*, 9789−9798.
(43) Chen, F.; Wu, Q.; Lü, Q.; Xu, Y.; Yu, Y. Synthesis and Characterization of Bifunctional Mesoporous Silica Adsorbent for Simultaneous Removal of Lead and Nitrate Ions. *Sep. Purif. Technol.* **2015**, *151*, 225−231.
(44) Lee, J. Y.; Chen, C. H.; Cheng, S.; Li, H. Y. Adsorption of Pb (II) and Cu (II) Metal Ions on Functionalized Large-Pore Mesoporous Silica. *Int. J. Environ. Sci. Technol.* **2015**, 1−12.
(45) Tang, Y.; Liang, S.; Wang, J.; Yu, S.; Wang, Y. Amino-Functionalized Core-Shell Magnetic Mesoporous Composite Microspheres for Pb(II) and Cd(II) Removal. *J. Environ. Sci.* **2013**, *25*, 830−837.
(46) Idris, S. A.; Davidson, C. M.; McManamon, C.; Morris, M. A.; Anderson, P.; Gibson, L. T. Large Pore Diameter MCM-41 and its Application for Lead Removal from Aqueous Media. *J. Hazard. Mater.* **2011**, *185*, 898−904.

DOI: 10.1021/acsami.5b06951
ACS Appl. Mater. Interfaces XXXX, XXX, XXX−XXX